Evidence of past migration of the ice divide between the Shirase and Sôya drainage basins derived from chemical characteristics of the marginal ice in the Sôya drainage basin, East Antarctica

Yoshinori IIZUKA,[1] Hideki MIURA,[2] Shogo IWASAKI,[3] Hideaki MAEMOKU,[4] Takanobu SAWAGAKI,[5] Ralf GREVE,[1] Hiroshi SATAKE,[6] Kimikazu SASA,[7] Yuki MATSUSHI[8]

[1]*Institute of Low Temperature Science, Hokkaido University, Sapporo 060-0819, Japan*
E-mail: iizuka@lowtem.hokudai.ac.jp
[2]*National Institute of Polar Research, 1-9-10 Kaga, Itabashi-ku, Tokyo 173-8515, Japan*
[3]*Management Section for Intellectual Property, Kitami Institute of Technology, 165 Koen-cho, Kitami 090-8507, Japan*
[4]*Graduate School of Education, Hiroshima University, 1-1-1 Kagamiyama, Higashi-Hiroshima 739-8524, Japan*
[5]*Graduate School of Environmental Science, Hokkaido University, Sapporo 060-0810, Japan*
[6]*Faculty of Science, University of Toyama, 3190 Gofuku, Toyama 930-8555, Japan*
[7]*Institute of Physics, University of Tsukuba, Ibaraki 305-8577, Japan*
[8]*Micro Analysis Laboratory, Tandem Accelerator, University of Tokyo, Tokyo 113-0032, Japan*

ABSTRACT. Ice originating near the inland ice divide of the ice sheet can reappear as marginal ice at the surface near the ice terminal in the ablation area. We have analyzed $\delta^{18}O$ values and ion concentrations of the Skallen, Skarvsnes and Hamna terminal ice sections, located along the estuary line in the Sôya drainage basin, East Antarctica. The data suggest that the upper part of the Skallen terminal ice section could have originated from inland precipitation on the Shirase drainage basin during marine isotope stage (MIS) 5e, while the upper part of Skarvsnes and Hamna terminal ice sections could have originated from inland precipitation on the Sôya drainage basin. We calculate past elevation maps for the Antarctic ice sheet using the three-dimensional model, SICOPOLIS. This model suggests that the upstream portion of the Sôya drainage basin during the glacial period (MIS 2, 3 or 4) was located to the northeast of its present location. A flow history is proposed wherein ice from the inland Shirase drainage area flowed over the present ice-divide line from the Shirase to the Sôya drainage basin during the glacial period. The ice in the Sôya drainage basin then flowed to the marginal part of the sheet after the ice divide had assumed its present position.

INTRODUCTION

The Antarctic ice sheet consists of several drainage basins, whose borders are called ice divides. Each basin represents a hydrological cycle: snow precipitates on the basin, ice flows to the margin, and ice discharges to the ocean. Ice originating near the inland ice divide can reappear at the surface near the ice terminal in the ablation area, where it can be easily sampled (Reeh and others, 1993). Because this ice passes near the bed at some points along its path to the surface, some details of the climatic record such as millennium-scale variations may be lost. However, the main features are preserved in the ice sheet (e.g. Reeh and others, 1993).

In Antarctica, ablation is mainly controlled by the dynamics of rapidly flowing ice streams, which promote carving and melting under ice shelves near the grounding line of the ice sheet (Rignot and Thomas, 2002; Rignot and others, 2008). Many of the ice streams are organized into a converging-type drainage basin along the flowline (Rignot and Thomas, 2002; Rignot and others, 2008). The remainder of the Antarctic ice sheet consists of spreading-type drainage basins, where the flow at the margin is relatively slow (e.g. Higashi, 1997). The edges of the spreading-type basins are therefore more likely to preserve ancient ice originating from inland precipitation. The present structure of the Antarctic ice sheet (drainage basin boundaries, present surface elevations, ice-divide distributions, etc.) is well known from satellite monitoring (e.g. H.J. Zwally and others, http://nsidc.org/data/gla12.html). Little is known, however, about the structure of the Antarctic ice sheet in the past. Relating the present migration of the ice divide to historical conditions requires a precise dynamical model of the ice sheet and an accurate evaluation of the mass balance.

The Shirase drainage basin feeds an ice stream whose rate of discharge is currently the second largest in Antarctica. The velocity of the ice stream at the Shirase drainage point is $\sim$2300 m a^{-1} (Nakawo and others, 1978; Fujii, 1981; Rignot, 2002; Nakamura and others, 2007). The Shirase drainage basin is gradually thinning (Naruse, 1979), so its dynamics are expected to fluctuate in the near future (e.g. Pattyn and Naruse, 2003; Nakamura and others, 2007). It converges to a marginal point wedged between the Harald and Sôya drainage basins (Higashi, 1997) which are both of the spreading type. The average marginal velocity of the Sôya drainage basin is less than a few m a^{-1}, except for a few small ice streams (Nakawo and others, 1978). The marginal ice of the Sôya drainage basin probably consists of ancient ice originating from inland precipitation around the Shirase and Sôya drainage basins.

The history of ice-sheet fluctuation at the Sôya coast shows an interesting variation within one drainage basin. The study of mollusc fossils (Miura and others, 1998) reveals the simultaneous retreat of the northern part of the ice sheet

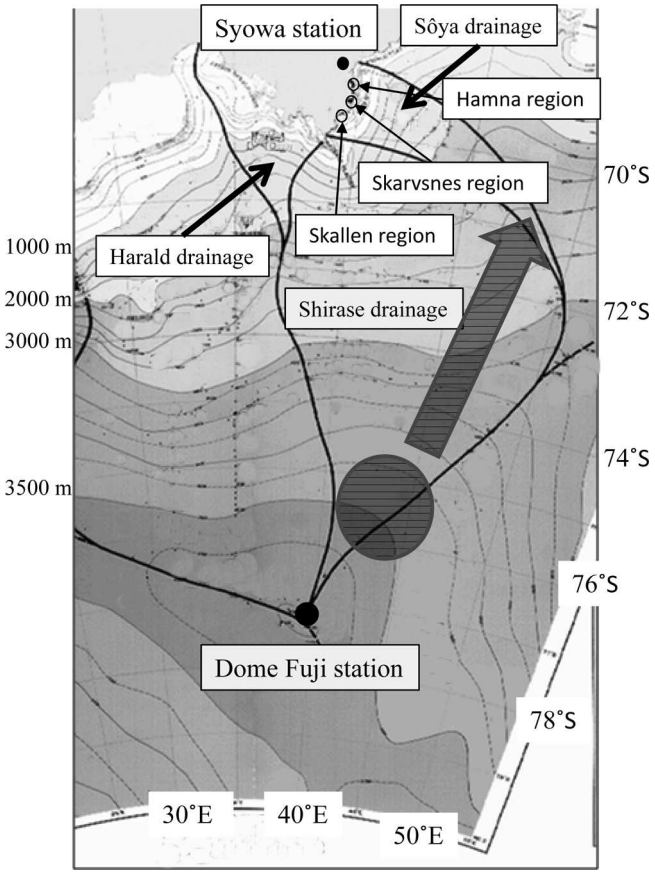

Fig. 1. Map of east Dronning Maud Land. The gray tones and contours indicate the surface elevation of the ice sheet, and the thick black curves are ice divides. This figure is adapted from a map in Higashi (1997). The black circle and thick arrow represent features of the flow history of the Skallen terminal ice.

and advance of the southern part during the Last Glacial Maximum (LGM). This suggests that the past ice-flow distribution (e.g. the ice-divide position) was different from the present distribution. Three-dimensional (3-D) ice-sheet models cannot precisely evaluate the past fluctuations of areas <100 km in length, due to their low spatial resolution. Thus, the flow history of ancient ice in the Sôya drainage basin may provide valuable clues to the past ice distribution on larger scales.

Stable-isotope and ion concentrations are useful tracers of the spatial distribution of accumulated polar ice (Reeh and others, 1993, 2002; Moore and others, 2006). In surface snow, these chemical compositions tend to increase linearly from inland to marginal regions (e.g. Satow and others, 1999; Suzuki and others, 2002). By analyzing stable oxygen isotope ratios and ion concentrations in the terminal ice of the Sôya drainage basin, we show that some of this ice originated from the inland Shirase drainage basin. Hence, we discuss how inland precipitation on the Shirase drainage basin could have flowed to the marginal Sôya drainage basin.

STUDY SITE AND ANALYTICAL PROCEDURES

The present Shirase drainage basin is ~1000 km in length along the central flowline. Its headstream is located at Dome Fuji station (77.4° S, 39.4° E; 3810 m a.s.l.), and its estuary at 70.2° S, 38.7° E (0 m a.s.l.) (Fig. 1). The maximum width of the Shirase drainage basin is ~450 km, which it reaches at ~3000 m a.s.l. Below this point, the Shirase drainage basin converges to the estuary and forms a rapidly flowing ice stream. The Sôya drainage basin neighbors the Shirase drainage basin to the east. At present, its length along the central flowline is ~500 km. Its headstream is located at 71.8° S, 50.4° E (3000 m a.s.l.) and eventually achieves a width of ~130 km along its estuary line, from 70.2° S, 38.7° E (0 m a.s.l.) to 68.8° S, 39.8° E (0 m a.s.l.) (Fig. 1). The ice divide between these two drainage basins controls the flow history of the accumulated snow around east Dronning Maud Land (EDML).

We sampled terminal ice from three regions in the Sôya drainage basin. The Skallen (69.6° S, 39.4° E), Skarvsnes (69.5° S, 39.6° E) and Hamna (69.3° S, 39.6° E) regions are located along the southern, central and northern parts of the 130 km estuary respectively (Fig. 1). Although the Sôya drainage basin has some small outlet ice streams, there are none in these three regions. The terminus of the ice sheet forms an ice cliff 10–30 m high (Fig. 2). The lower part of the ice cliff is an exposed, debris-laden ice layer. The stratigraphic sequence of the basal layer is uniform in the neighborhood of each sampling site. The debris probably originates from subglacial bedrock, since there are no nunataks on the upper reaches of the terminal ice, just a widespread white ice sheet.

The Skallen, Skarvsnes and Hamna terminal ice sections were sampled in the winters of 2006, 2004 and 1994 respectively, by the Japanese Antarctic Research Expeditions. A columnar section was cut from the ice cliff using a chainsaw. All sections contain a debris-laden ice layer and overlying white glacier ice. The frozen samples were transported to a cold laboratory in the Institute of Low Temperature Science and preserved below –20°C.

We measured the concentrations of dissolved ions and the stable $\delta^{18}O$ isotope at ~100 mm intervals in the Skallen, Skarvsnes and Hamna terminal ice sections, and conducted a stratigraphic analysis. After melting in a pre-cleaned pack, ice samples were filtered with a pore size of 0.45 μm. Using an ion chromatograph (Dionex 500) we then analyzed the filtered liquid for seven major soluble ions: Cl^-, NO_3^-, SO_4^{2-}, Na^+, K^+, Mg^{2+} and Ca^{2+}. The estimated errors in these concentrations are <5%. We measured isotope concentrations using the CO_2 equilibration method, with mass spectrometers at the National Institute of Polar Research (MAT252) and Toyama University (PRISM). The estimated errors in these data are <0.1‰ for $\delta^{18}O$. Chemical data for the Hamna terminus ice have been published by Iizuka and others (2000, 2001).

RESULTS

The Skallen terminus ice

Figure 3a shows the complete sequence of ice and debris strata observed in the Skallen terminus ice. It also indicates the height profiles of $\delta^{18}O$ and some ion (Cl^-, Na^+ and Ca^{2+}) concentrations. The horizontal axis of this figure represents the height measured upward from the base of the ice sheet; this convention is used for the remainder of the paper.

The debris-rich layer extends from 0.84 to 1.80 m in height. The Na^+ and Ca^{2+} profiles show a similar trend, namely that they are much higher within this layer than in precipitated ice from EDML (Satow and others 1999; Suzuki and others 2002) even during the cold climatic stages

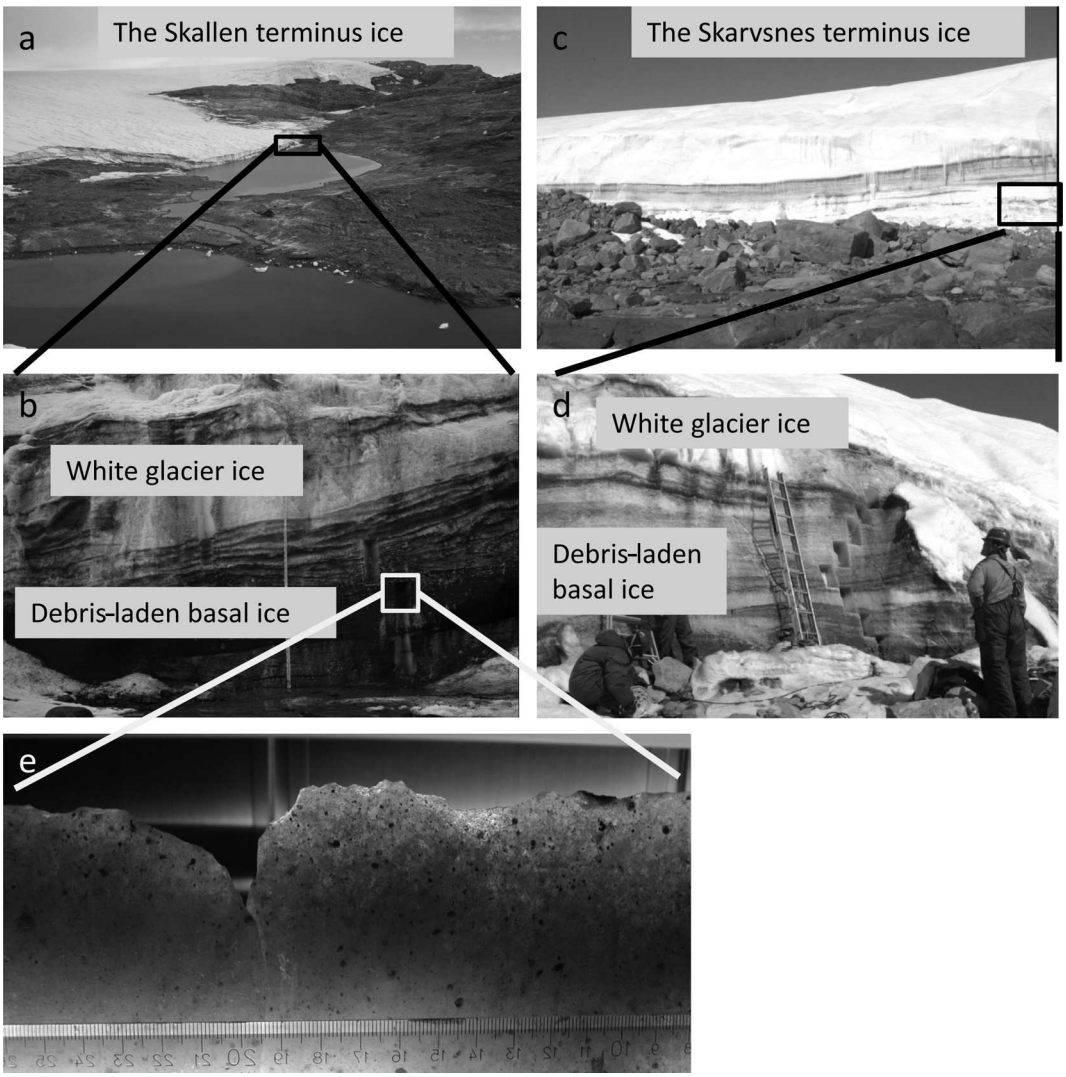

Fig. 2. The sampling sites. (a) Aerial view of the Skallen terminal region. The black rectangle indicates the sampling site. (b) Scaled-up view of the sampling site in (a). The white glacier ice seems to have black debris, but this debris is present only on the surface. (c) Aerial view of the Skarvsnes terminus ice. The black rectangle indicates the sampling site. (d) Scaled-up view of the sampling site in (c). Views of the Hamna terminus ice are provided by Iizuka and others (2001). (e) Photograph of the Skallen basal ice section, taken at the location of the white square in (b). This ice section has a great deal of debris and one of the highest Ca^{2+} concentrations (Fig. 3) in the Skallen basal ice. The black spots are debris from the base of the ice sheet. The grayish color of the ice is due to light scattering from a high bubble concentration.

(Watanabe and others, 2003). Looking at the data in more detail, we find that both Na^+ and Ca^{2+} are strongly correlated with the debris concentration ($r^2 = 0.78$). These results suggest that the primary source of Na^+ and Ca^{2+} is dissolution from subglacial bedrock debris. The SO_4^{2-}, K^+ and Mg^{2+} profiles are all similar to the Na^+ and Ca^{2+} profiles.

$\delta^{18}O$ ranges from –52‰ to –20‰. The $\delta^{18}O$ values change abruptly on crossing the upper border of the debris-rich layer at 1.84 m. The upper part of the ice core (1.84–4.81 m) has the lowest average value of $\delta^{18}O$, -51.7 ± 0.6‰ (Table 1). The lower layers (0–1.84 m) of the sample have high $\delta^{18}O$ values, with an upper limit of –20‰ and an average of 35.7 ± 10.5‰ (Table 1). Even if the Skallen terminus ice experienced some fractionation due to refreezing at the inland bedrock, the $\delta^{18}O$ value should change by no more than several per mil (e.g. Souchez and Jouzel, 1984). Thus, the difference between the upper and lower profiles can be attributed mainly to differences in the $\delta^{18}O$ of the precipitation. The Cl^- concentration profile is similar to the $\delta^{18}O$ profile, their correlation coefficient being relatively high ($r^2 = 0.80$). This result suggests that the primary source of Cl^- is not debris dissolution but sea salt from the atmosphere. In general, the continental crust seldom contains chlorine. The upper (1.84–4.81 m) and lower (0–1.84 m) parts of the sample have average Cl^- concentrations of 1.67 ± 1.00 and 7.06 ± 2.93 μmol L^{-1} respectively (Table 1).

In the upper part of the Skallen terminus, the white glacier ice and the debris-laden basal ice have similar $\delta^{18}O$ values and Cl^- concentrations (Table 1). We therefore integrate these data in the following discussion.

The Skarvsnes terminus ice

Figure 3b shows a complete stratigraph of the Skarvsnes terminus ice, along with the height profiles of $\delta^{18}O$ and some ion (Cl^-, Na^+, Ca^{2+}) concentrations.

There are some thin (several cm or less), debris-rich layers in the Skarvsnes terminus ice, although the total amount of debris present is less than that observed in the Skallen terminus. The Ca^{2+} concentration is much higher than in

Table 1. Average $\delta^{18}O$ values (‰) and average concentrations of seven ions (μmol L^{-1}) in the Skallen, Skarvsnes and Hamna terminal ice sections

	$\delta^{18}O$	Cl^-	NO_3^-	SO_4^{2-}	Na^+	K^+	Mg^{2+}	Ca^{2+}
Skallen terminal ice								
White glacier ice ($n=12$)	–52.3	1.53	0.55	0.74	1.32	0.29	0.19	0.47
Upper part ice ($n=40$)	–51.7	1.67	0.34	2.00	2.71	3.92	1.81	32.71
Lower part ice ($n=30$)	–35.7	7.06	0.12	9.11	21.92	26.12	18.68	346.25
Skarvsnes terminal ice								
White glacier ice ($n=1$)	–47.5	1.65	0.12	0.15	1.88	0.36	0.17	0.43
Upper part ice ($n=44$)	–46.4	1.71	0.30	1.83	3.36	5.94	2.81	24.44
Lower part ice ($n=6$)	–42.5	6.99	0.87	4.40	13.87	14.79	5.49	78.88
Hamna terminal ice								
White glacier ice ($n=2$)	–45.9	1.31	0.51	0.52	1.26	0.03	0.15	0.15
Upper part ice ($n=66$)	–45.8	0.59	0.12	0.78	1.62	2.04	1.90	9.45
Lower part ice ($n=24$)	–46.7	2.72	0.05	2.78	10.94	9.33	4.16	34.77

precipitated ice from EDML (Satow and others 1999; Suzuki and others, 2002; Watanabe and others, 2003), so the primary source of Ca^{2+} in these layers is probably dissolution from subglacial bedrock debris.

$\delta^{18}O$ ranges from –48‰ to –37‰, changing dramatically at a height of 0.39 m. Above this point (0.39–3.89 m), the average $\delta^{18}O$ value is -46.4 ± 1.4‰. Below this point (0–0.39 m), the average $\delta^{18}O$ value is 42.5 ± 2.5‰ (Table 1). The upper part (0.39–3.89 m) and the lower part (0–0.39 m) have average Cl^- concentrations of 1.71 ± 1.25 and 6.99 ± 5.29 μmol L^{-1} respectively (Table 1), comparable to those observed in precipitated ice from inland EDML. As with the Skallen terminus ice, we can conclude that the Cl^- in the Skarvsnes terminus ice originates mainly from atmospheric sea salt.

The upper (0.39–3.89 m) and lower (0–0.39 m) parts of the sample have average Na^+ concentrations of 3.36 ± 2.08 and 13.87 ± 10.12 μmol L^{-1} respectively (Table 1). On average, assuming that all Cl^- ions came from sea salt, we expect non-sea-salt Na to account for 46.9% and 52.7% of the Na^+ in the upper and lower parts respectively, of the Skarvsnes terminus ice. Meteoric nssNa in precipitation contributes at most 30% to the overall Na concentration, even during the LGM when terrestrial sodium was most prevalent (Röthlisberger and others, 2002). Thus, contributions of $nssNa^+$ higher than 30% indicate that the Skarvsnes terminus ice contains ions from both atmospheric sea salt and subglacial debris dissolution.

The white glacier ice and debris-laden basal ice have similar $\delta^{18}O$ values and Cl^- concentrations in the upper part of the Skarvsnes terminus (Table 1). Thus, as with the Skallen ice, we integrate these data in the following discussion.

The Hamna terminus ice

Figure 3c shows a complete stratigraphy of the Hamna terminus ice and indicates the height profiles of $\delta^{18}O$ and some ion (Cl^-, Na^+, Ca^{2+}) concentrations. As with the Hamna terminus ice, the chemical characteristics of this sample are reported elsewhere (Iizuka and others, 2000, 2001). In summary, the Hamna terminus ice can be divided into upper (1.30–7.50 m) and lower (0–1.30 m) parts with different characteristics. The primary source of Na^+ and Ca^{2+} is dissolution from subglacial bedrock debris. As with the two other sites, the primary source of Cl^- is atmospheric sea salt. The average $\delta^{18}O$ values and Cl^- concentrations in ice from the upper part, including white glacier ice, are -45.8 ± 0.7‰ and 0.59 ± 0.39 μmol L^{-1} respectively (Table 1).

DISCUSSION

Origin of the upper part of the Skallen, Skarvsnes and Hamna terminus samples

Here we focus on the upper parts of the Skallen, Skarvsnes and Hamna terminus ice sections. Their average $\delta^{18}O$ values are –51.7‰, –46.4‰ and –45.8‰ respectively. These are very low values compared with precipitation from the marginal region of the Sôya drainage basin, where seasonal $\delta^{18}O$ values range from –33‰ to –10‰ at present (Kato, 1979). This indicates that the basal ice originated from precipitation on the inland regions of the Shirase and Sôya drainage basins.

Figure 4 plots $\delta^{18}O$ values against Cl^- concentrations for the three terminal ice sections and present surface snow. Also shown are data representing this relationship during the corresponding climatic period of the Dome Fuji (DF) ice core. The DF ice core was drilled at the summit of the Shirase drainage basin, and covers several glacial and interglacial periods (e.g. Watanabe and others, 2003). In general, cold-stage ice has lower $\delta^{18}O$ values and higher Cl^- concentrations than warm-stage ice (Figs 4 and 5). Typically, Cl^- concentrations are >3 μmol L^{-1} in the cold stages (marine isotope stages (MIS) 2 and 4) but <2 μmol L^{-1} in the warm stages (MIS 1, 5a, 5c and 5e) (Figs 4 and 5). At present, Cl^- concentrations vary little over the inland region above 2500 m a.s.l. (e.g. Suzuki and others, 2002) where $\delta^{18}O$ values are less than –40‰. Figure 4 indicates that all three terminal ice sections have $\delta^{18}O$ values less than –40‰ and Cl^- concentrations of ~2 μmol L^{-1}, suggesting that the three terminal ices originate from inland precipitation during a warm climatic period (e.g. MIS 1, 5a, 5c and 5e).

The above suggestion is supported by the average Na^+ concentrations in white glacier ice of the three termini (Table 1), which are <2 μmol L^{-1}. The main source of Na^+ is also sea salt (1.18 for the sea-salt ratio of Cl^-/Na^+), and the Na^+ concentrations of the Sôya and Shirase drainage basins above 2500 m a.s.l. fall below 2 μmol L^{-1} (e.g. Suzuki and others, 2002) only during warm climatic periods such as MIS 1, 5a, 5c and 5e (Watanabe and others, 2003). Thus, the Na^+

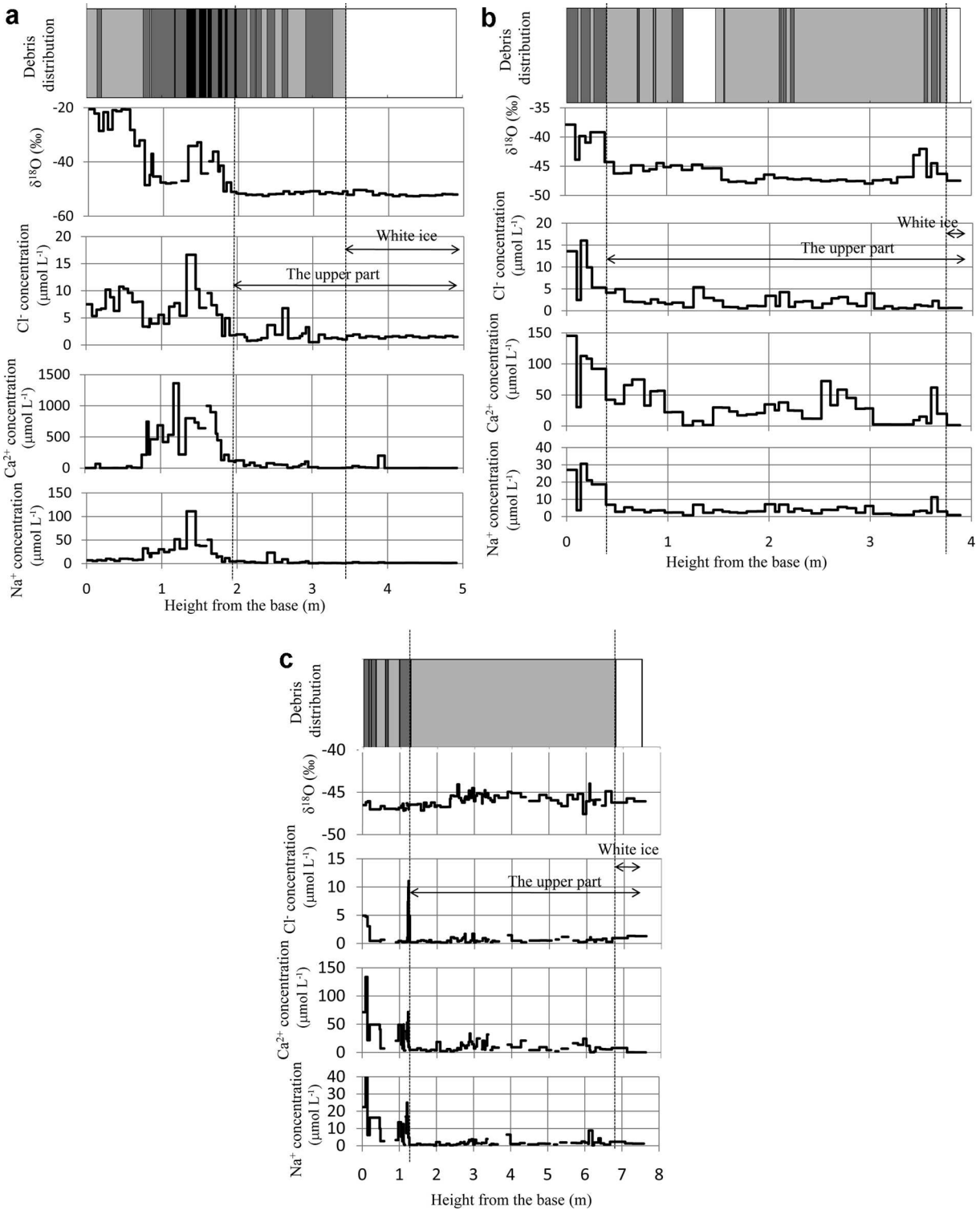

Fig. 3. (a) Profiles of the debris distribution, $\delta^{18}O$ values and Cl^-, Na^+ and Ca^{2+} concentrations of the Skallen terminal ice. White, light gray, heavy gray, and black marks indicate zero, low, medium and high levels of debris respectively. (b, c) Same as (a), but for the Skarvsnes and Hamna terminal ice respectively.

in this ice also originates from inland precipitation during a warm climatic period.

The average $\delta^{18}O$ values observed in the MIS 1, 5a, 5c and 5e sections are also within ±3‰ of the present Dome Fuji $\delta^{18}O$ value (Figs 4 and 5). The relationship between $\delta^{18}O$ and surface elevation (Satow and Watanabe, 1992) is

$$\delta^{18}O\ (‰) = 0.01188E - 11.04\ (r^2 = 0.98),$$

where E is elevation (m). If we assume that the present spatial distribution of $\delta^{18}O$ in EDML has not changed since previous climatic periods (MIS 1, 5a, 5c and 5e), then the upper parts of the Skallen, Skarvsnes and Hamna terminus

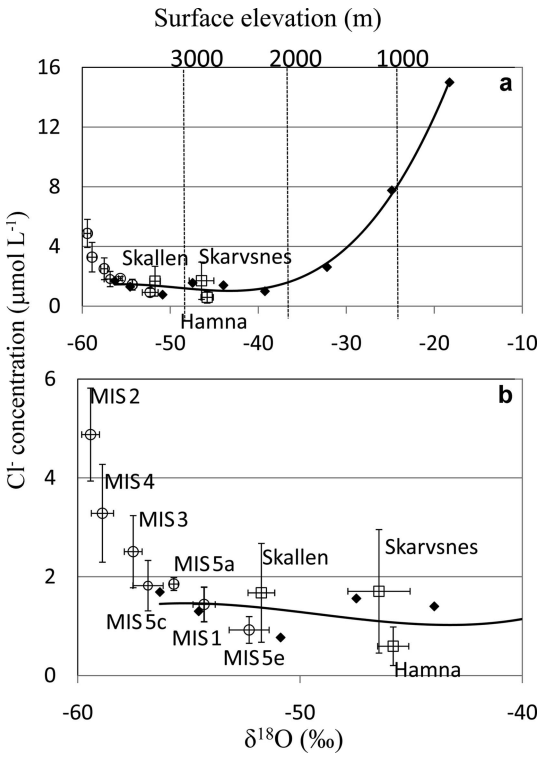

Fig. 4. (a) The relationship between $\delta^{18}O$ values and Cl^- concentrations for ice around EDML. (b) A close-up of the same plot for low $\delta^{18}O$ values and Cl^- concentrations. The average values of the upper parts of the Skallen, Skarvsnes and Hamna terminal ice sections are shown by open squares. The average values in snow from the surface to 2 m depth obtained from nine altitudes are shown by black diamonds. An approximate fit is shown by the black curve. The average values of past climatic stages (MIS 1, 2, 3, 4, 5a, 5c and 5e) are shown by open circles. The surface snow and past ice data are taken from Higashi (1997) and Watanabe and others (2003) respectively.

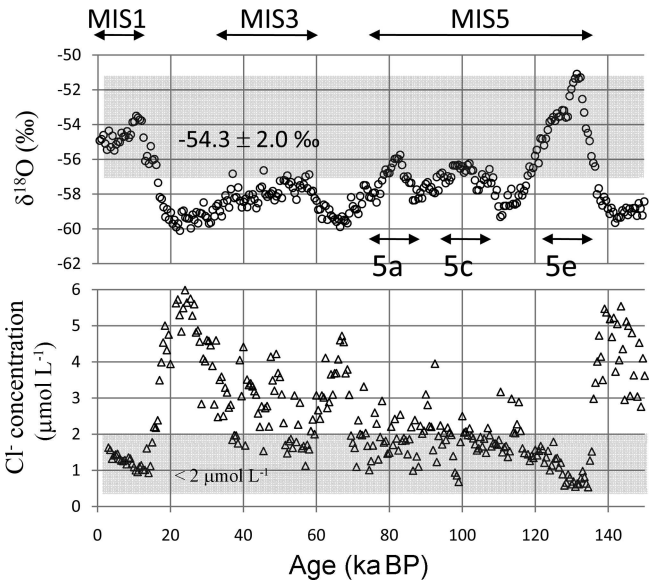

Fig. 5. $\delta^{18}O$ values and Cl^- concentrations in the most recent 150 ka BP of the DF ice core, as reported by Watanabe and others (2003). The gray shaded areas of each component correspond to the upper part of the terminal ice sections.

ice sections could have originated from inland precipitation around 3423 ± 253, 2976 ± 253 and 2926 ± 253 m a.s.l. respectively. Note that the precipitation originates from higher elevations in the southern sample area (Skallen), and from lower elevations in the northern sample area (Hamna).

Since the present head of the Sôya drainage basin is ~3000 m a.s.l. (Fig. 1), precipitation in the Skallen terminal ice section must have originated from the neighboring Shirase drainage basin which lies at a higher elevation. As a reference, the amplitude of the altitude change does not exceed 150 m on the Antarctic Plateau over the last 420 ka BP (Ritz and others, 2001). This result implies that the ice divide between the Shirase and Sôya drainage basins was different in the past, and that ice presently located in the terminal part of the Sôya drainage basin originated from different past precipitation. On the other hand, the precipitation in the Skarvsnes and Hamna terminal ice section must have originated from the top of the Sôya drainage basin. This result implies that the past ice divide between the Shirase and Sôya drainage basins was located between the Skallen and Skarvsnes regions.

Deducing the age of the upper Skallen terminal ice by principal component analysis

The upper part of the Skallen terminal ice originates from inland precipitation on the Shirase drainage basin. Here we deduce the age of the upper part of the Skallen terminal ice by a principal component analysis (PCA) of its chemical data, $\delta^{18}O$ values and Cl^-, NO_3^-, SO_4^{2-}, Na^+, Mg^{2+} and Ca^{2+} concentrations. Time series of these values have already been derived from the DF ice core over the most recent 150 ka BP (Watanabe and others, 2003). The six ions are the most common species in the DF core (Iizuka and others, 2008). Note that the K^+ concentration in the DF ice core is so small (Watanabe and others, 2003) that it is occasionally absent from the ion chromatogram, and so was left out of the PCA.

After smoothing the DF series by a 500 year running mean, we were left with 284 data points. Along with 12 independent chemical analyses of white glacial ice from the Skallen terminus, the smoothed chemical vectors from the DF core are then projected onto a new basis of seven principal components.

Figure 6 plots the second principal component against the first for each vector in the dataset. Each climatic stage of the DF ice core is given a different symbol, as is the Skallen ice. We calculated average values for the seven components and subtracted these from the data to give deviations around zero. The eigenvalues (and contributions) of the first and second components are 5.87 (83.9%) and 0.59 (8.5%) respectively; together they explain 92.4% of the total variance. Figure 6 suggests that the first component is closely related to air temperature, because it is positive during MIS 1 and 5e and negative during MIS 2 and 4. The meaning of the second component is not obvious, but it probably depends on the ratio of Ca^{2+} (terrestrial material) and Na^+ (sea salt). The MIS 1 and 5e periods are interglacial, with low Ca^{2+} and Na^+ concentrations. The MIS 2, 3 and 4 periods are relatively cold glacial, with high Ca^{2+} and Na^+ concentrations. MIS 5a–5d are relatively warm glacial, with low Ca^{2+} but high Na^+ concentrations.

Several climatic stages can be distinguished clearly by their position in Figure 6, and each stage forms a distinct cluster indicating consistent chemical characteristics and

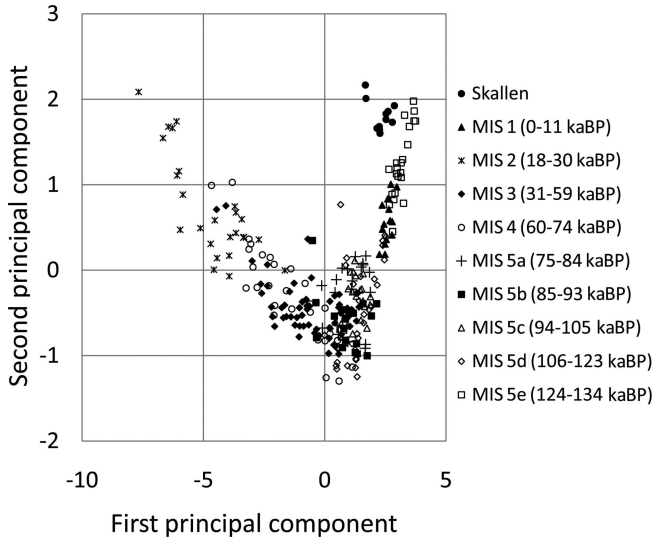

Fig. 6. The first two principal components of chemical data from the white glacier ice of the Skallen terminal ice and each climatic stage of the DF ice core.

$\delta^{18}O$ values. The Skallen terminal ice is positioned near the MIS 5e cluster but far from the MIS 1, 5a and 5c clusters. This analysis strongly suggests that the upper part of the Skallen terminal ice originates in MIS 5e precipitation, and rules out MIS 1, 5a and 5c.

If we take into account a simple flow model (Nye, 1963) of an ice sheet 3000 m thick with 50 mm of annual accumulation (precipitation giving rise to the Skarvsnes and Hamna terminal ice), the thicknesses of annual layers located at one-half and three-quarters of the total height are 25 and 13 mm respectively. These layers are disturbed as they flow to the terminus by various dynamic processes (e.g. folding, boudinage, and faulting near the bedrock) (Paterson, 1994). The marginal ice sections are several meters thick, with a sampling resolution of about 100 mm, corresponding to a period of several decades and a resolution of several years. This terminal period corresponds to a single datum of the DF ice core (Fig. 5). The relatively low resolution is sufficient to transform the annual layer concentrations into a well-homogenized series, with smooth stochastic peaks. Thus, estimations from the ice-flow model allow us to relate the $\delta^{18}O$ values and Cl^- concentrations of the marginal ice samples to recent climatic stages in the DF ice core as described above.

Past migrations of the ice divide between the Shirase and Sôya drainage basins

In order to deduce the past position of the ice divide between the Shirase and Sôya drainage basins, we calculate the past elevation of the Antarctic ice sheet using a large-scale ice-sheet model. SICOPOLIS (SImulation COde for POLythermal Ice Sheets) is a commonly used 3-D dynamic/thermodynamic model developed by Greve (1995, 1997) and available as free software (http://sicopolis.greveweb.net). We conducted a paleoclimatic simulation from 422 ka BP until the present, adopting a spatial resolution of 40 km. Greve (http://hdl.handle.net/2115/34433) provides details of the simulation set-up.

The main outputs used in this study are snapshot elevation maps of the Antarctic ice sheet at 140, 130, 84, 66, 45, 20, 9 and 0 ka BP, corresponding to typical MIS 6, 5e, 5a, 4, 3, 2, 1 and present conditions. These ages cover fluctuations of the ice sheet during the most recent glacial–interglacial period. Figure 7 shows some of these elevation maps. We compared the 0 ka BP elevation map calculated by SICOPOLIS with the present elevation distributions (Higashi, 1997), and found flexion points on the 2400 and 2600 m contours of EDML in both distributions (Figs 7 and 8). The 2400 and 2600 m flexion points are located on the right and left banks of the Sôya drainage ice divide respectively. We confirmed that the 2400 and 2600 m flexion points at 140, 130, 84, 66, 45, 20 and 9 ka BP are also located on the right and left banks of the Sôya drainage ice divide. Hence, these two features can serve as useful reference points to determine past fluctuations of the ice divide. We measured changes in the latitude and longitude of the 2400 and 2600 m flexion points with respect to their present locations in each snapshot.

Since SICOPOLIS does not take into account the dynamics of an ice shelf, the past elevation distributions of the marginal part have an undetermined margin of error. By choosing our reference points from the inland part of the Sôya drainage basin, we avoided this source of error.

Table 2 describes the migration of the 2400 and 2600 m flexion points. At 140, 84, 66, 45 and 20 ka BP (MIS 2, 3, 4 and 6), during the glacial period, these points were situated to the northeast of their present locations. For example, the 2400 and 2600 m points at 20 ka BP (MIS 2) are located at 0.12° N, 0.37° E and 0.14° N, 0.46° E with respect to their present positions (two-way arrow in Fig. 7). In particular, the rapid eastward migration (by 0.46° E) of the 2600 m point means that the 20 ka BP ice divide was located in the present center of the Sôya drainage basin (Fig. 8).

This is how precipitated ice can have flowed from physical coordinates now located in the Shirase drainage basin to the terminus of the present Sôya drainage basin. Before the eastward migration of the ice divide, the west side of the region now comprising the Sôya drainage basin consisted of inland Shirase drainage ice (black enclosure in Fig. 8). After the ice divide migrated to its present position, ice originally located in the Shirase drainage basin became part of the Sôya drainage basin and flowed toward the Sôya coast. The northeastward migration also explains why only the Skallen region, located close to the central estuary of the past Shirase drainage basin, stores ice from an ice divide farther upstream. The Skallen and Skarvsnes regions are located farther from the divide, so their compositions are less affected by its past migration.

The SICOPOLIS software also outputs the surface velocity of the ice sheet. Using these data, we can calculate a lower limit for the age of the terminal ice. We began tracking the flow from the inferred origin of Skallen marginal ice, at 74.6° S, 47.0° E (3400 m a.s.l.). The surface velocity at this position is about 5 m a^{-1}. Moving along the flowline toward the Skallen region, we obtain velocities of >10 m a^{-1} at 70.8° S, 47.3° E, and >100 m a^{-1} at 70.1° S, 42.1° E. Integrating along this path, we find that the total flow time from the origin to the Skallen region is about 98 ka. As the surface velocity is higher than the particle velocity within the ice sheet, we can take 98 ka as a lower limit. This calculation supports the PCA result, which implies that the upper part of the Skallen terminal ice was precipitated during MIS 5e (124–134 ka BP). This calculation rules out the MIS 1 and MIS 5a stages.

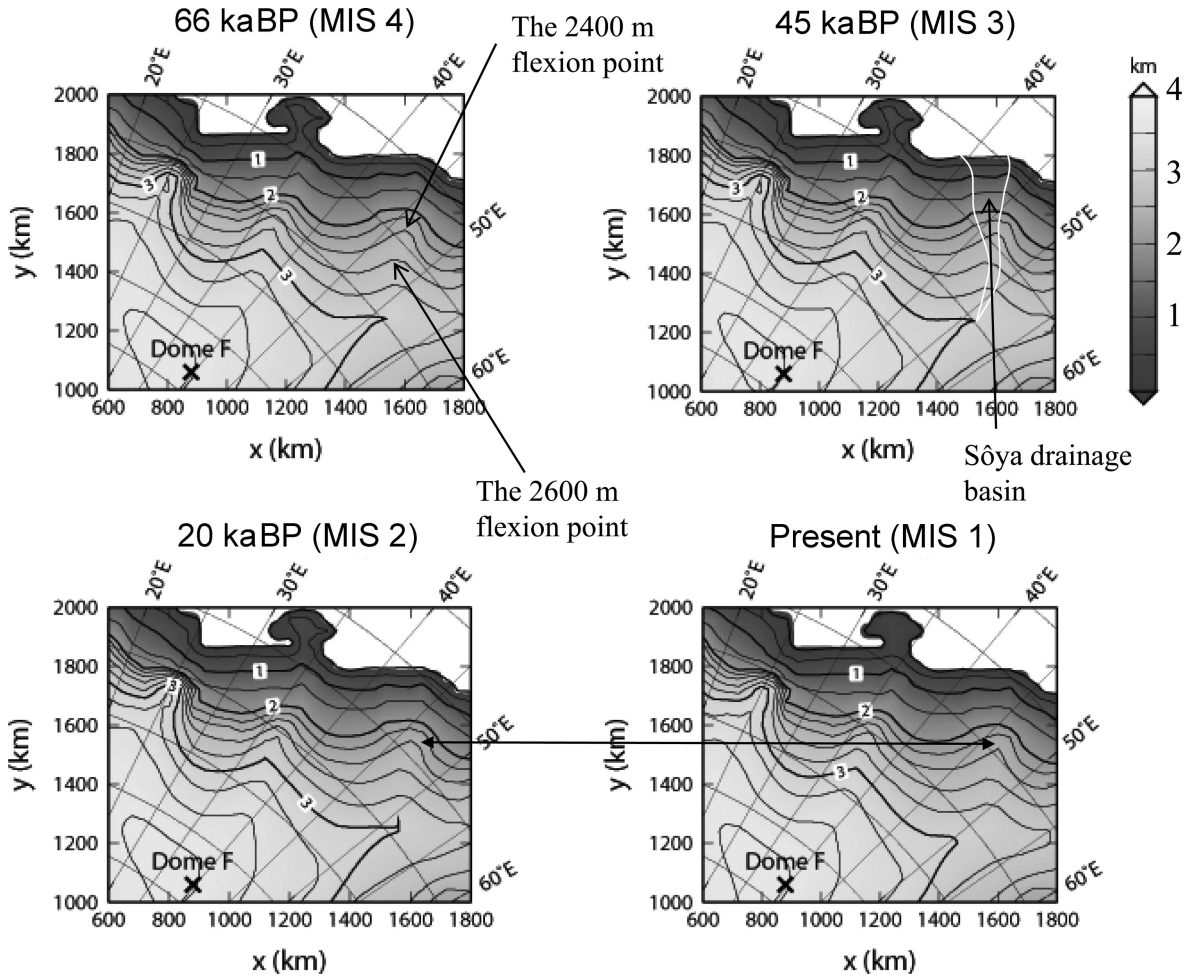

Fig. 7. Some snapshots of past ice elevations of the Antarctic ice sheet (66, 45, 20 and 0 ka BP) calculated by SICOPOLIS. The arrow between the MIS 2 and present snapshots shows an example of the moving of flexion points.

Table 2. Past migrations of the 2400 and 2600 m flexion points relative to their present positions

Flexion point	Migration	
ka BP	°N	°E
2400 m		
140 (MIS 6)	0.15	0.47
130 (MIS 5.5)	0.00	0.00
84 (MIS 5.1)	–0.02	–0.06
66 (MIS 4)	0.08	0.24
45 (MIS 3)	0.09	0.27
20 (MIS 2)	0.12	0.37
9 (Holocene)	–0.01	–0.03
0 (present)	0.00	0.00
2600 m		
140 (MIS 6)	0.19	0.62
130 (MIS 5.5)	0.03	0.11
84 (MIS 5.1)	0.03	0.10
66 (MIS 4)	0.10	0.33
45 (MIS 3)	0.10	0.32
20 (MIS 2)	0.14	0.46
9 (Holocene)	0.01	0.02
0 (present)	0.00	0.00

Flow history and formation mechanism of the Skallen terminal ice

The above results and discussion allow us to propose a detailed flow history of the Skallen terminal ice in the Sôya drainage basin. Figures 1 and 7 describe the history of the upper ice, which could originate in precipitation during a warm period of MIS 5e over the inland area of the Shirase drainage basin at about 3423 m a.s.l. (black circle in Fig. 1). The precipitated ice then flowed *over* the present ice-divide line between the Shirase and Sôya drainage basins (black arrow in Fig. 1) at a time when the ice divide was to the northeast of its present location (MIS 2, 3 or 4) (black enclosure in Fig. 8). Finally, the ice flowed through the Sôya drainage basin to the Skallen region after the ice divide moved to its present position (MIS 1; black arrow in Fig. 8).

This flow history implies that the Shirase drainage basin of the glacial period, one of the fastest discharges of the Antarctic ice sheet, is narrower than it once was. Further analysis of terminal ice taken from other parts of the Sôya and Harald drainage basins will allow a more precise evaluation of mass balance and ice dynamics in Shirase Glacier.

Sometime during the aforementioned flow history, the upper part of the basal ice layer (1.84–3.48 m) would have touched the bedrock, although the white glacier ice (3.48–4.81 m) did not. The $\delta^{18}O$ of the lower part of the basal ice (0–0.56 m) is at most –20‰, corresponding to the annual

average in local precipitation at the Sôya coast. Thus, the lower part of the Skallen basal ice consists of on-site precipitation. Two mechanisms may have caused the inland ice (the upper part) to overlap the local ice (the lower part) near the bedrock. First, the lower part was already dead ice when the Skallen terminal ice passed over it. In this case, the inland ice could have obducted on the dead ice by thrusting. Second, the lower part was formed from local summer meltwater, which froze at the base of the ice sheet and adhered to the underside of the inland ice.

The $\delta^{18}O$ of the boundary between the upper and lower parts of the basal ice (0.56–1.84 m) is between –48‰ and –28‰. These values suggest that the boundary layer was formed by mixing inland ice and local ice. The boundary layer has a high Ca^{2+} concentration and a significant amount of debris, which may have been entrained by ice forming at the interface between ice sheet and bed. Figure 2e shows a transmissive photograph of the boundary layer ice, which consists of bubbly ice and contains dispersed (Lawson, 1979) or clotted (Knight, 1997) debris facies. Knight (1997) suggested that such debris types have traveled long and far since their entrainment in the basal ice, which if true would imply that the boundary layer formed inland somewhere other than the present Skallen region. On the other hand, if the basal ice formed by freezing meltwater, it should consist of bubble-free ice (e.g. Knight, 1997; Iizuka and others, 2001). We conclude that the lower part of the basal ice already existed as dead ice of local precipitation when the Skallen terminal ice advanced through its original location. The upper part was then obducted on the dead ice by thrusting.

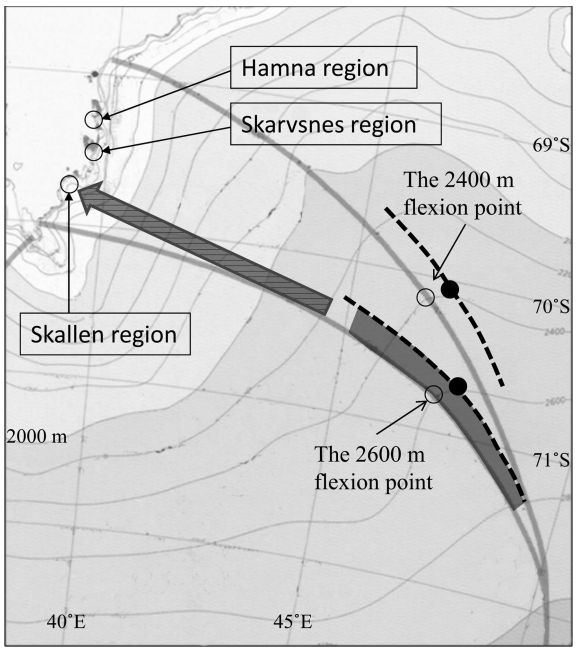

Fig. 8. A scaled-up map of the Sôya drainage basin from Figure 1. The locations of the 2400 and 2600 m flexion points at 20 ka BP are indicated by black circles. The two dotted lines are the reconstructed ice divides at 20 ka BP obtained by processing parallel shifts from the present ice divides.

CONCLUSION

We have measured $\delta^{18}O$ values and six ion concentrations in sections of terminal ice taken from the Skallen, Skarvsnes and Hamna regions of the Sôya drainage basin, located in the southern, central and northern parts of the 130 km estuary respectively. We calculated past elevation maps of the Antarctic ice sheet using the 3-D SICOPOLIS model. The $\delta^{18}O$ values and Cl^- concentrations suggest that the upper parts of the Skallen ice sections, consisting of white glacier and debris-laden basal ice, could have originated from inland precipitation in a region occupied by the present-day Shirase drainage basin ($\sim 3423 \pm 252$ m a.s.l.). On the other hand, precipitation ice in the Skarvsnes and Hamna termini must have originated from the top of the Sôya drainage basin. These results imply that the ice divide between the Shirase and Sôya drainage basins was once located between the Skallen and Skarvsnes regions. PCA of chemical signatures from the Skallen ice section and the DF core suggests that the inland precipitation that created the Skallen terminus occurred during a warm period of MIS 5e. The past elevation maps suggest that the upstream region of the Sôya drainage basin was located to the northeast of its present position during the glacial period (MIS 2, 3 or 4). From this information, we reconstructed a flow history wherein precipitated ice of the inland Shirase drainage area flowed over the present ice-divide line from the Shirase to the Sôya drainage basin, at a time when the ice divide was located farther to the northeast than it is at present. The ice on the Sôya drainage basin then flowed to the terminal part after the ice divide assumed its present position. This history implies that the Shirase drainage basin, one of the fastest discharges of the Antarctic ice sheet, was wider during the last glacial period than it is at present.

We have also suggested a formation mechanism for the Skallen terminal ice. In contrast to the upper part of the Skallen basal ice, the lower part consists of on-site precipitation. Because the boundary-layer ice contains bubbles and debris facies typical of long travel, the basal ice probably existed as dead ice of local precipitation when the Skallen terminal ice passed overhead. The upper part of the basal layer was then obducted on the dead ice by thrusting, in a manner typical of ice dynamics observed in the Shirase and Sôya drainage basins.

ACKNOWLEDGEMENTS

We thank the Japanese Antarctic Research Expedition (JARE-35, -45 and -47) for sampling the terminal ice sections. The paper was significantly improved as a result of comments by V. Morgan and an anonymous referee, and by the Scientific Editor Wei Li Wang, to whom we are greatly indebted. This study was supported by Scientific Research (B) grant No. 21710002 provided by Japan's Ministry of Education, Culture, Sports, Science and Technology (MEXT) and the Japan Society for the Promotion of Science (JSPS). R. Greve was supported by a Grant-in-Aid for Scientific Research A (No. 22244058) from the JSPS and by a Category 2 research grant from the Institute of Low Temperature Science (ILTS), Sapporo, Japan.

REFERENCES

Fujii, Y. 1981. Aerophotographic interpretation of surface features and estimation of ice discharge at the outlet of the Shirase drainage basin, Antarctica. *Antarct. Rec.* 72, 1–15.

Greve, R. 1995. Thermomechanisches Verhalten polythermer Eisschilde – Theorie, Analytik, Numerik. (PhD thesis, Technische Hochschule Darmstadt.)

Greve, R. 1997. Application of a polythermal three-dimensional ice sheet model to the Greenland ice sheet: response to steady-state and transient climate scenarios. *J. Climate,* **10**(5), 901–918.

Higashi, A., *ed.* 1997. *Antarctica: East Queen Maud Land–Enderby Land glaciological folio*. Tokyo, National Institute of Polar Research.

Iizuka, Y., M. Igarashi, T. Shiraiwa, R. Naruse, T. Yamada and O. Watanabe. 2000. Chemical characteristics of basal ice near Hamna Icefall, East Antarctica. *Polar Meteorol. Glaciol.,* **14**, 8–15.

Iizuka, Y., H. Satake, T. Shiraiwa and R. Naruse. 2001. Formation processes of basal ice at Hamna Glacier, Sôya Coast, East Antarctica, inferred by detailed co-isotopic analyses. *J. Glaciol.,* **47**(157), 223–231.

Iizuka, Y. *and 6 others*. 2008. A relationship between ion balance and the chemical compounds of salt inclusions found in the Greenland Ice Core Project and Dome Fuji ice cores. *J. Geophys. Res.,* **113**(D7), D07303. (10.1029/2007JD009018.)

Kato, K. 1979. Oxygen isotopic composition of fallen snow in Antarctica. *Antarct. Rec.* 67, 124–135. [In Japanese with English summary.]

Knight, P.G. 1997. The basal ice layer of glaciers and ice sheets. *Quat. Sci. Rev.,* **16**(9), 975–993.

Lawson, D.E. 1979. Sedimentological analysis of the western terminus region of the Matanuska Glacier, Alaska. *CRREL Rep.* 79-9.

Miura, H., H. Maemoku, K. Seto and K. Moriwaki. 1998. Late Quaternary East Antarctic melting event in the Soya Coast region based on stratigraphy and oxygen isotopic ratio of fossil molluscs. *Polar Geosci.,* **11**, 260–274.

Moore, J.C. *and 7 others*. 2006. Interpreting ancient ice in a shallow ice core from the South Yamato (Antarctica) blue ice area using flow modeling and compositional matching to deep ice cores. *J. Geophys. Res.,* **111**(D16), D16302. (10.1029/2005JD006343.)

Nakamura, K., K. Doi and K. Shibuya. 2007. Estimation of seasonal changes in the flow of Shirase Glacier using JERS-1/SAR image correlation. *Polar Sci.,* **1**(2–4), 73–83.

Nakawo, M., Y. Ageta and A. Yoshimura. 1978. Discharge of ice across Sôya Coast. *Mem. Natl Inst. Polar Res.,* Special Issue 7, 235–244.

Naruse, R. 1979. Thinning of the ice sheet in Mizuho Plateau, East Antarctica. *J. Glaciol.,* **24**(90), 45–52.

Nye, J.F. 1963. Correction factor for accumulation measured by the thickness of the annual layers in an ice sheet. *J. Glaciol.,* **4**(36), 785–788.

Paterson, W.S.B. 1994. *The physics of glaciers. Third edition.* Oxford, etc., Elsevier.

Pattyn, F. and R. Naruse. 2003. The nature of complex ice flow in Shirase Glacier catchment, East Antarctica. *J. Glaciol.,* **49**(166), 429–436.

Reeh, N., H. Oerter and H. Miller. 1993. Correlation of Greenland ice-core and ice-margin $\delta(^{18}O)$ records. *In* Peltier, W.R., *ed. Ice in the climate system*. Berlin, etc., Springer-Verlag, 481–497. (NATO ASI Series I: Global Environmental Change 12.)

Reeh, N., H. Oerter and H.H. Thomsen. 2002. Comparison between Greenland ice-margin and ice-core oxygen-18 records. *Ann. Glaciol.,* **35**, 136–144.

Rignot, E. 2002. Mass balance of East Antarctic glaciers and ice shelves from satellite data. *Ann. Glaciol.,* **34**, 217–227.

Rignot, E. and R.H. Thomas. 2002. Mass balance of polar ice sheets. *Science,* **297**(5586), 1502–1506.

Rignot, E. *and 6 others*. 2008. Recent Antarctic ice mass loss from radar interferometry and regional climate modelling. *Nature Geosci.,* **1**(2), 106–110.

Ritz, C., V. Rommelaere and C. Dumas. 2001. Modeling the evolution of Antarctic ice sheet over the last 420,000 years: implications for altitude changes in the Vostok region. *J. Geophys. Res.,* **106**(D23), 31,943–31,964.

Röthlisberger, R. *and 6 others*. 2002. Dust and sea salt variability in central East Antarctica (Dome C) over the last 45 kyrs and its implications for southern high-latitude climate. *Geophys. Res. Lett.,* **29**(20), 1963. (10.1029/2002GL015186.)

Satow, K. and O. Watanabe. 1992. Distribution of mean $\delta^{18}O$ values of surface snow layers and their dependence on air temperature in Enderby Land–East Queen Maud Land, Antarctica. *Proc. NIPR Symp. Polar Meteorol. Glaciol.,* **5**, 120–127.

Satow, K., O. Watanabe, H. Shoji and H. Motoyama. 1999. The relationship among accumulation rate, stable isotope ratio and surface temperature on the plateau of east Dronning Maud Land, Antarctica. *Polar Meteorol. Glaciol.,* **13**, 43–52.

Souchez, R.A. and J. Jouzel. 1984. On the isotopic composition in δD and $\delta^{18}O$ of water and ice during freezing. *J. Glaciol.,* **30**(106), 369–372.

Suzuki, T., Y. Iizuka, K. Matsuoka, T. Furukawa, K. Kamiyama and O. Watanabe. 2002. Distribution of sea salt components in snow cover along the traverse route from the coast to Dome Fuji station 1000 km inland at east Dronning Maud Land, Antarctica. *Tellus,* **54B**(4), 407–411.

Watanabe, O. *and 10 others*. 2003. General tendencies of stable isotopes and major chemical constituents of the Dome Fuji deep ice core. *Mem. Natl Inst. Polar Res.,* Special Issue 57, 1–24.

MS received 8 September 2009 and accepted in revised form 21 April 2010